Available online at www.sciencedirect.com
ScienceDirect
Nuclear Physics A 967 (2017) 856–859
NUCLEAR PHYSICS A
www.elsevier.com/locate/nuclphysa

$p\Xi^-$ Correlation in Relativistic Heavy Ion Collisions with Nucleon-Hyperon Interaction from Lattice QCD

Tetsuo Hatsuda[1], Kenji Morita[2], Akira Ohnishi[2], Kenji Sasaki[2]

[1] *iTHEMS Program and Nishina Center, RIKEN, Saitama 351-0198, Japan*

[2] *Yukawa Institute for Theoretical Physics, Kyoto University, Kyoto 606-8502, Japan*

Abstract

On the basis of the $p\Xi^-$ interaction extracted from (2+1)-flavor lattice QCD simulations at the physical point, the momentum correlation of p and Ξ^- produced in relativistic heavy ion collisions is evaluated. $C_{\rm SL}(Q)$ defined by a ratio of the momentum correlations between the systems with different source sizes is shown to be largely enhanced at low momentum due to the strong attraction between p and Ξ^- in the $I = J = 0$ channel. Thus, measuring this ratio at RHIC and LHC and its comparison to the theoretical analysis will give a useful constraint on the $p\Xi^-$ interaction.

Keywords: exotic dibaryon, hyperon-nucleon force, Lattice QCD

1. Introduction

The coupled-channel Nambu-Bethe-Salpeter (NBS) wave function measured in lattice QCD [1, 2] can now provide "theoretical" information of hyperon-nucleon and hyperon-hyperon interactions through the HAL QCD method [3, 4, 5, 6]. The energy-independent non-local potentials $U(r, r')$ obtained by the method allow us to calculate the scattering phase shifts and binding energies of two baryons.

These potentials are also useful for analyzing the two-particle momentum correlations in relativistic heavy ion collisions [7]. It was recently studied in [8] that the possible spin-2 $p\Omega^-$ dibaryon state suggested by lattice QCD [9] can be probed by the $p\Omega^-$ momentum correlation at RHIC and LHC. In particular, the ratio of correlation functions between small and large collision systems, $C_{\rm SL}(Q)$, is shown to be a good measure to extract the strong interaction effect without much contamination from the Coulomb effect [8]. In the present paper, we extend the analysis to the $p\Xi^-$ system in $I = J = 0$ channel which was recently predicted to have large attraction by the lattice QCD simulations at physical quark masses [4].

2. Lattice QCD formulation

We start with the normalized four-point function R in channel α defined by

$$R^{\alpha}(\vec{r}, t) \quad \equiv \quad \frac{\langle 0 \mid B_{\alpha_1}(\vec{x}+\vec{r}, t) B_{\alpha_2}(\vec{x}, t)\, \overline{\mathcal{J}}(0) \mid 0 \rangle}{\sqrt{Z_{\alpha_1} Z_{\alpha_2}} \exp[-(m_{\alpha_1} + m_{\alpha_2})t]}, \qquad (1)$$

http://dx.doi.org/10.1016/j.nuclphysa.2017.04.041

where $B_{\alpha_1}(\vec{x},t)$ and $B_{\alpha_2}(\vec{x},t)$ are the sink operators for octet baryons. $\sqrt{Z_{\alpha_1}}\ \sqrt{Z_{\alpha_2}}$ are the corresponding wave-function renormalization factors, and $\mathcal{J}(0)$ is a source operator at zero initial-time to create two baryons. The coupled channel potential is obtained through the linear partial differential equation [2];

$$\left(D_t^\alpha - H_0^\alpha\right) R^\alpha(\vec{r},t) \quad = \quad \int d^3r'\ U^{\alpha\beta}(\vec{r},\vec{r}')\Delta^{\alpha\beta}R^\beta(\vec{r}',t), \tag{2}$$

with $H_0{}^\alpha = -\frac{\nabla^2}{2\mu^\alpha}$ and $\Delta^{\alpha\beta} = \exp[-(m_{\beta_1}+m_{\beta_2})t]/\exp[-(m_{\alpha_1}+m_{\alpha_2})t]$. D_t^α is a time-derivative operator whose leading-order term reads $-\partial/\partial t$. We introduce a derivative expansion to treat the non-local potential as

$$U^{\alpha\beta}(\vec{r},\vec{r}') = (V_{\rm LO}^{\alpha\beta}(\vec{r}) + V_{\rm NLO}^{\alpha\beta}(\vec{r}) + \cdots)\delta(\vec{r}-\vec{r}'). \tag{3}$$

In the following, we truncate the expansion at the leading order.

We employ (2 + 1)-flavor QCD configurations on the $L^4 = 96^4$ lattice with the lattice spacing $a \simeq 0.085$fm. This corresponds to the physical size, $La = 8.1$fm, which guarantees that the finite volume effect on $U^{\alpha\beta}(\vec{r},\vec{r}')$ is negligible. The quark masses are chosen for the system to be almost at the physical point; $m_\pi \simeq 146$ MeV and $m_K \simeq 525$ MeV [4]. The total number of configurations is 414×4 space-time rotations $\times$ 48 wall sources. The baryon masses measured in this setup are listed below.

baryon	N	Λ	Σ	Ξ
mass [MeV]	953 ± 7	1123 ± 3	1204 ± 2	1332 ± 1

3. $p\Xi^-$ potential in $I = 0$ channel

The $S = -2$ baryon-baryon interactions including the I=0 $\Lambda\Lambda - N\Xi - \Sigma\Sigma$ coupled-channel system have been recently reported in [4]. In particular, one of the diagonal components $V_{N\Xi,N\Xi}(r)$ in the $(I,J) = (0,0)$ channel ($^1S_0$) was shown to have large attractive well at intermediate distance and relatively weak repulsive core at short distance, while $V_{N\Xi,N\Xi}(r)$ in the $(I,J) = (0,1)$ channel ($^3S_1$) has weaker attractive well and stronger repulsive core. Also, $V_{N\Xi,N\Xi}(r)$ in the $I = 1$ channels do not have appreciable attraction. Motivated by these observations, we parametrize the lattice results of $V_{N\Xi,N\Xi}(r)$ in the $I = 0$ channels by a combination of the Gauss and Yukawa functions as shown in Fig.1. Curves with different t correspond to the potentials obtained from $R(\vec{x},t)$ for different t, so that the t dependence of $V(r)$ reflects typical magnitude of the systematic error of the lattice data. We found that the strong QCD attraction in Fig.1(Left) together with the Coulomb attraction leads to the $^1S_0$ system close to the unitary region where the inverse of the scattering length is close to zero. On the other hand, the $^3S_1$ system described by Fig.1(Right) has strong repulsion even with the Coulomb attraction.

4. $p\Xi^-$ momentum correlation

The correlation function of non-identical pair such as $p\Xi^-$ is given in terms of the two-particle distribution $N_{p\Xi}(\mathbf{k}_p,\mathbf{k}_\Xi)$ normalized by a product of the single particle distributions, $N_\Xi(\mathbf{k}_\Xi)N_p(\mathbf{k}_p)$,

$$C(\mathbf{Q},\mathbf{K}) \equiv \frac{N_{p\Xi}(\mathbf{k}_p,\mathbf{k}_\Xi)}{N_p(\mathbf{k}_p)N_\Xi(\mathbf{k}_\Xi)} \simeq \frac{\int d^4x_p \int d^4x_\Xi\ S_p(x_p,\mathbf{k}_p)S_\Xi(x_\Xi,\mathbf{k}_\Xi)\left|\Psi_{p\Xi}(\mathbf{r}')\right|^2}{\int d^4x_p\ S_p(x_p,\mathbf{k}_p)\int d^4x_\Xi\ S_\Xi(x_\Xi,\mathbf{k}_\Xi)},$$

where relative and total momenta are defined as $\mathbf{Q} = (m_p\mathbf{k}_\Xi - m_\Xi\mathbf{k}_p)/M$ and $\mathbf{K} = \mathbf{k}_p + \mathbf{k}_\Xi$, respectively, with $M \equiv m_p + m_\Xi$. The source functions $S_i(x_i,\mathbf{k}_i) \equiv E_i\frac{dN_i}{d^3\mathbf{k}_i d^4x_i}$ (with $i = p,\Xi$ and $E_i = \sqrt{\mathbf{k}_i^2 + m_i^2}$) correspond to the phase space distributions of p and Ξ at freeze-out. The final state interaction after the freeze-out is described by the two-particle wave function $\Psi_{p\Xi}$ with a shifted relative coordinate $\mathbf{r}' = \mathbf{x}_\Xi - \mathbf{x}_p - \mathbf{K}(t_p - t_\Xi)/M$.

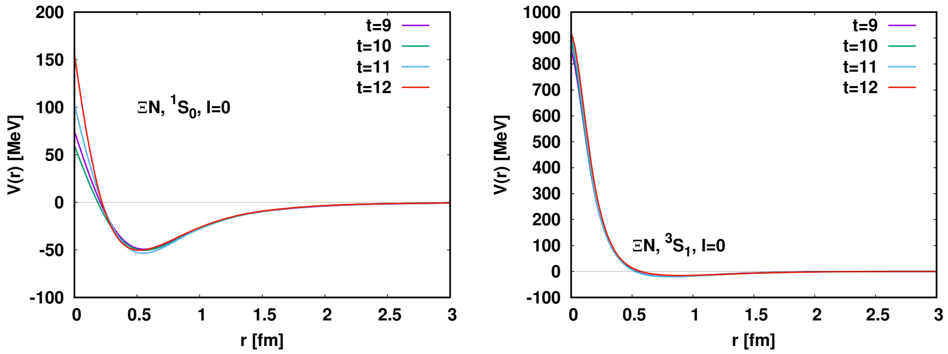

Fig. 1. The $N\Xi$ potentials in the $I = 0$ channel fitted to the (2+1)-flavor lattice QCD data at the physical point. Euclidean time used for extracting the lattice QCD potential is denoted by t. (Left) The potential in the $(I, J) = (0, 0)$ channel ($^1S_0$). (Right) The potential in the $(I, J) = (0, 1)$ channel ($^3S_1$).

Here we consider the static source function with spherical symmetry to extract the essential part of physics;

$$S_i(x_i, \mathbf{k}_i) \propto E_i\, e^{-\frac{\mathbf{x}_i^2}{2R_i^2}}\, \delta(t - t_i), \quad (i = p, \Xi^-), \tag{4}$$

where R_i is a source size parameter. Assuming the equal-time emission $t_p = t_\Xi$, we obtain

$$C(Q) = \int [dr] \int \frac{d\Omega}{4\pi} |\psi^C(\mathbf{r})|^2 + \frac{1}{8} \int [dr] \left(|\chi_{\rm sc}^{\rm J=0}(r)|^2 - |\psi_0^C(r)|^2 \right) + \frac{3}{8} \int [dr] \left(|\chi_{\rm sc}^{\rm J=1}(r)|^2 - |\psi_0^C(r)|^2 \right), \tag{5}$$

where $[dr] = \frac{1}{2\sqrt{\pi}R^3} dr\, r^2 e^{-\frac{r^2}{4R^2}}$ with $R = \sqrt{(R_p^2 + R_\Xi^2)/2}$ being the effective size parameter. $\int d\Omega$ is the integration over the solid angle between $\mathbf{Q}$ and $\mathbf{r}$. Note that $\psi^C(\mathbf{r})$ is the Coulomb wave function characterized by the reduced mass and the Bohr radius of the $p\Xi^-$ system. Its S-wave component is denoted by $\psi_0^C(r)$. The scattering wave functions obtained by solving the Schrödinger equation with both strong interaction and Coulomb interaction are denoted by $\chi_{\rm sc}^{J=0}(r)$ and $\chi_{\rm sc}^{J=1}(r)$ for the $^1S_0$ channel and $^3S_1$ channel, respectively. We assume that the $I = 1$ sector does not contribute substantially to $C(Q)$, which is supported by the fact that the $I = 1$ $p\Xi^-$ potential has only short-range repulsion [4]. The factors $1/8 = 1/2\times1/4$ and $3/8 = 1/2\times3/4$ originate from the isospin and spin multiplicities. Also, we assume that the absorptive contribution by the coupling to the $\Lambda\Lambda$ channel is negligible since it is reported to be weak due to its short range nature [4].

In [8], the "SL (small-to-large) ratio" was introduced: It is defined as a ratio of $C(Q)$ between the systems with different source sizes,

$$C_{\rm SL}(Q) \equiv C_{R_{p,\Xi}=2.5{\rm fm}}(Q)/C_{R_{p,\Xi}=5{\rm fm}}(Q), \tag{6}$$

which has good sensitivity to the strong interaction without much contamination from the Coulomb interaction [8]. Shown in Fig.2 is $C_{\rm SL}(Q)$ of the $p\Xi^-$ system with the Coulomb interaction under the assumption of the static source given in Eq.(4).

The large enhancement of this ratio at small Q originates from the fact that the $p\Xi^-$ system in the $^1S_0$ channel is close to the unitary region. The result has rather weak dependence on t, which indicates that the systematic errors of the lattice data do no affect the final results significantly. We have also checked that taking the expanding source as discussed in [8] does not change the present result.

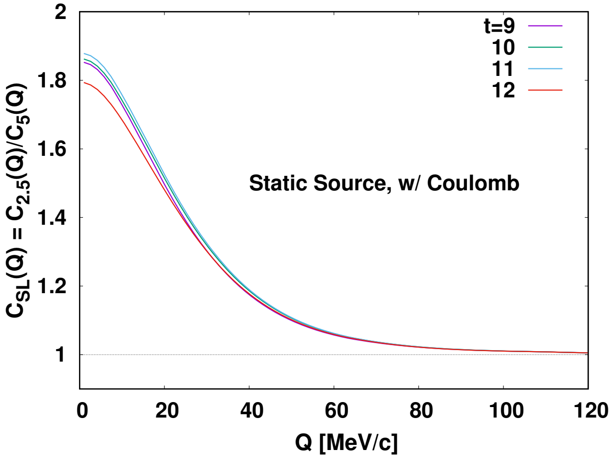

Fig. 2. SL (small-to-large) ratio $C_{\rm SL}(Q)$ for the momentum correlation of $p\Xi^-$ system as a function of the relative momentum Q in the case of the static source. Both the strong and Coulomb interactions are taken into account for the $p\Xi^-$ interaction. Different curves correspond to different potentials shown in Fig.1.

5. Summary

The momentum correlation of the $p\Xi^-$ system was presented by employing the $p\Xi^-$ potential extracted from the coupled channel analysis of the (2+1)-flavor lattice QCD data at the physical point. So-called the SL-ratio of the momentum correlation ($C_{\rm SL}(Q)$) was calculated and was shown to have large enhancement at small Q due to the strong attraction between p and Ξ^- in the ${}^1S_0$ channel. Measuring this ratio at RHIC and LHC and its comparison to the present theoretical analysis will give useful constraint on the $p\Xi^-$ interaction. Such information is particularly important not only for the nature of the possible H-dibaryon coupled to $p\Xi^-$ [4] but also for the properties of Ξ-hypernuclei [10] and for Ξ^- in the central core of the neutron star [11].

Acknowledgments

This work is supported in part by MEXT Grant-in-Aid for Scientific Research (JP15K17667, 24105008), SPIRE (Strategic Program for Innovative REsearch) Field 5 project and "Priority Issue on Post-K computer" (Elucidation of the Fundamental Laws and Evolution of the Universe). K.M. was supported by JSPS Grant 16K05349, and National Science Center, Poland under grants:, Maestro DEC-2013/10/A/ST2/00106. T.H. was partially supported by RIKEN iTHES Project and iTHEMS Program. The authors thank HAL QCD Collaboration for proving us with the data for $p\Xi^-$ interactions and for stimulating discussions.

References

[1] N. Ishii, S. Aoki and T. Hatsuda, Phys. Rev. Lett. **99** (2007) 022001 [nucl-th/0611096].
[2] N. Ishii *et al.* [HAL QCD Collaboration], Phys. Lett. B **712** (2012) 437 [arXiv:1203.3642 [hep-lat]].
[3] T. Doi *et al.* [HAL QCD Collaboration], PoS LATTICE **2016** (2017) 110 [arXiv:1702.01600 [hep-lat]].
[4] K. Sasaki *et al.* [HAL QCD Collaboration], PoS LATTICE **2016** (2017) 116 [arXiv:1702.06241 [hep-lat]].
[5] N. Ishii *et al.* [HAL QCD Collaboration], PoS LATTICE **2016** (2017) 127 [arXiv:1702.03495 [hep-lat]].
[6] H. Nemura *et al.* [HAL QCD Collaboration], PoS LATTICE **2016** (2017) 101 [arXiv:1702.00734 [hep-lat]].
[7] S. Cho *et al.* [ExHIC Collaboration], arXiv:1702.00486 [nucl-th].
[8] K. Morita, A. Ohnishi, F. Etminan and T. Hatsuda, Phys. Rev. C **94** (2016) 031901 [arXiv:1605.06765 [hep-ph]].
[9] F. Etminan *et al.* [HAL QCD Collaboration], Nucl. Phys. A **928** (2014) 89 [arXiv:1403.7284 [hep-lat]].
[10] K. Nakazawa *et al.*, PTEP **2015** (2015) 033D02.
[11] see e.g. a review, G. Baym, T. Hatsuda, T. Kojo, C. J. Pethick, P. D. Powell, Y. Song, and T. Takatsuka, (in preparation).